

## ORIGIN OF MAGNETIC FIELD IN THE INTRACLUSTER MEDIUM: PRIMORDIAL OR ASTROPHYSICAL?

JUNGYEON CHO<sup>1</sup>*Draft version October 9, 2014*

## ABSTRACT

The origin of magnetic fields in clusters of galaxies is still an unsolved problem, which is largely due to our poor understanding of initial seed magnetic fields. If the seed magnetic fields have primordial origins, it is likely that large-scale pervasive magnetic fields were present before the formation of the large-scale structure. On the other hand, if they were ejected from astrophysical bodies, they were highly localized in space at the time of injection. In this paper, using turbulence dynamo models for high magnetic Prandtl number fluids, we find constraints on the seed magnetic fields. The hydrodynamic Reynolds number based on the Spitzer viscosity in the intracluster medium (ICM) is believed to be less than  $O(10^2)$ , while the magnetic Reynolds number can be much larger than that. In this case, if the seed magnetic fields have primordial origins, they should be stronger than  $O(10^{-11})$ G, which is very close to the upper limit of  $O(10^{-9})$ G set by the cosmic microwave background (CMB) observations. On the other hand, if the seed magnetic fields were ejected from astrophysical bodies, any seed magnetic fields stronger than  $O(10^{-9})$ G can safely magnetize the intracluster medium. Therefore, it is less likely that primordial magnetic fields are the direct origin of present-day magnetic fields in the ICM.

*Subject headings:* intergalactic medium — galaxies: magnetic fields — magnetohydrodynamics (MHD) — turbulence

## 1. INTRODUCTION

Observations have it that magnetic fields of order  $\mu$ G are present in clusters of galaxies (see, for example, Kronberg 1994; Zweibel & Heiles 1997; Carilli & Taylor 2002; Widrow 2002; Govoni & Feretti 2004; Vogt & Enßlin 2005; Ferrari et al. 2008; Ryu et al. 2012). No physical effect, e.g. a battery effect, seems to produce such strong magnetic fields directly. Therefore, it is natural to assume that weak seed magnetic fields were produced at some time and they have been amplified later to current strengths. According to this point of view, the origin of cosmic magnetism now involves two separate issues: generation of the initial seed magnetic fields and their amplification. In this paper, we try to find constraints on the seed magnetic fields by studying their amplification.

Theoretically, it is possible to generate weak magnetic fields in the early universe before the recombination (see Widrow et al. 2012 and references therein). However, it is highly unclear whether or not they have survived in the early universe and have become the seeds for present-day magnetic fields in the intracluster medium (ICM). Probably, one of the best-known mechanisms for producing cosmic seed magnetic fields is the Biermann battery effect (Biermann 1950), which should operate during the formation of the large-scale structure and can produce a seed field of order  $10^{-20}$ G. If seed magnetic fields were produced either in the early universe or during the large-scale structure formation, it is likely that the seed fields were spatially homogeneous on the scale of galaxy clusters.

Magnetic fields expelled from astrophysical bodies can also seed the ICM. First stars (Pudritz & Silk 1989;

Schleicher et al. 2010) or active galaxies (Hoyle 1969; Rees 1987; Daly & Loeb 1990; Kronberg et al. 2001) can inject magnetized materials into the intergalactic space. Galactic winds, supernova explosions, ram pressure stripping can also provide magnetized materials to the intergalactic space (see, for example, Rephaeli 1988; Kronberg 1994; Carilli & Taylor 2002; Donnert et al. 2009; Arieli et al. 2011). If a seed magnetic field was provided by an astrophysical object, it is likely that the seed magnetic field was spatially localized at the time of injection. As time goes on, the seed magnetic field can be dispersed away from the source and ultimately fill the whole system more or less homogeneously. If the homogenization timescale is greater than the Hubble time, it is possible to distinguish the primordial and the astrophysical origins of cosmic magnetism by observing intermittency of magnetic field distribution.

Turbulence is commonly observed in clusters and filaments in simulations of the large-scale structure formation (Kulsrud et al. 1997; Ryu et al. 2008; Xu et al. 2010; Vazza et al. 2011; Miniati 2014). Turbulence can provide an efficient mechanism for amplification of weak seed magnetic fields. In usual astrophysical environments, the magnetic diffusivity is very small, which enforces fluid elements and magnetic field lines move together. Therefore, chaotic turbulent motions can stretch magnetic field lines, making the magnetic field's strength and energy increase (Batchelor 1950; Zel'dovich et al. 1984; Childress & Gilbert 1995). This process is called small-scale turbulence dynamo.

Study of small-scale turbulence dynamo has a long history (e.g. Batchelor 1950; Kazantsev 1968; Vainstein & Ruzmaikin 1972; Pouquet et al. 1976; Meneguzzi et al. 1981; Kulsrud & Anderson 1992; Cho & Vishniac 2000; Haugen et al. 2004; Brandenburg & Subramanian 2005; Schekochihin & Cowley 2007; Cho et al. 2009; Beresnyak

<sup>1</sup> Department of Astronomy and Space Science, Chungnam National University, Daejeon, Korea; jcho@cnu.ac.kr

2012; Brandenburg et al. 2012; Schober et al. 2012a; Bovino et al. 2013; Yoo & Cho 2014). Most of the studies on the turbulence dynamo deal with growth of a uniform or a homogeneous seed magnetic field in a fluid with unit magnetic Prandtl number  $Pr_m$ , which is defined as  $\nu/\eta$ , where  $\nu$  is the viscosity and  $\eta$  is the magnetic diffusivity. Nevertheless, there are also studies for growth of localized seed magnetic fields (Molchanov et al. 1985; Ruzmaikin et al. 1989; Cho & Yoo 2012; Cho 2013) in unit magnetic Prandtl number turbulence and for growth of a uniform seed magnetic field in high magnetic Prandtl number turbulence (Schekochihin et al. 2004; Subramanian et al. 2006; Schekochihin & Cowley 2007; Bovino et al. 2013).

In this paper, we consider growth of both uniform and localized seed magnetic fields in high magnetic Prandtl number turbulence. We will argue that, when we adopt turbulence dynamo models for high magnetic Prandtl number fluids, astrophysical seed magnetic fields are more likely sources of magnetic fields in the ICM. In Section 2, we discuss turbulence dynamo in the ICM. In Section 3, we describe numerical methods and, in Section 4, we present the results. In Sections 5 and 6, we give discussions and summary, respectively.

## 2. TURBULENCE DYNAMO IN HIGH MAGNETIC PRANDTL NUMBER FLUIDS

If the hydrodynamic Reynolds number,  $Re \equiv Lv/\nu$ , where  $L$  is the outer scale of turbulence and  $v$  is the r.m.s. velocity) is very large, turbulence dynamo is so efficient that any seed magnetic fields follow virtually the same evolutionary track after a very short initial exponential growth stage (see Appendix). Therefore, in this case, it is difficult to find a constraint on the strength of the initial seed magnetic field. However, it is believed that  $Re$  in the ICM does not exceed  $O(10^2)$ . In this case, turbulence dynamo may not be so efficient and the strengths of the seed field may matter. In this section, we discuss turbulence dynamo in fluids with  $Re < O(10^2)$ . Note that, because the magnetic diffusivity is expected to be still very small in the ICM, the magnetic Prandtl number,  $Pr_m$ , can be much larger than unity (i.e.  $\nu \gg \eta$ ).

### 2.1. The hydrodynamic Reynolds number, $Re$ , in the ICM

Due to low density and high temperature, the mean free path between collisions,  $l_{mfp}$ , is very large and, therefore, the viscosity, which is approximately  $l_{mfp}$  times the particle velocity, may not be negligibly small in the ICM. Estimates for  $Re$  in cool cores and hot ICM, do not exceed  $O(10^2)$  (Robinson 2004; Ruszkowski et al. 2004; Reynolds et al. 2005; Brandenburg & Subramanian 2005; Schekochihin & Cowley 2006; Brunetti & Lazarian 2007) if we use the Spitzer (1962) formula for the viscosity.

In fact, the hydrodynamic Reynolds number for the central  $\sim 400$  kpc region of a cluster can be

$$Re \approx 28 \left( \frac{v}{400 \text{ km/s}} \right) \left( \frac{L}{400 \text{ kpc}} \right) \left( \frac{k_B T}{8 \text{ keV}} \right)^{-2.5} \left( \frac{n}{0.001 \text{ cm}^{-3}} \right) \left( \frac{\ln \Lambda}{40} \right) \quad (1)$$

(modified from Equation (2) in Brunetti & Lazarian

2007), where  $n$  is the number density,  $k_B$  is the Boltzmann constant,  $T$  is the temperature, and  $\ln \Lambda$  is the Coulomb logarithm. In this paper, we mainly assume that  $Re \lesssim O(10^2)$  in the ICM.

### 2.2. Theoretical expectations

If  $Re \lesssim 10^2$ , the viscous-cutoff wavenumber  $k_d$ , at which the velocity spectrum drops quickly due to viscous damping, is not much larger than the driving wavenumber. Therefore, the eddy turnover time at the viscous-cutoff scale is not much different from the large-scale eddy turnover time  $L/v$ , which makes turbulence dynamo inefficient. Because of inefficient turbulent dynamo, the strength of the initial seed magnetic field becomes important. In this section we consider turbulence dynamo in fluids with high magnetic Prandtl numbers<sup>2</sup>.

At the exponential growth stage, the magnetic field lines are stretched by turbulent motions at the viscous-cutoff scale, also known as the Kolmogorov scale. Since the viscous-cutoff scale is close to the outer scale of turbulence in high magnetic Prandtl number fluids, the kinetic energy density at the viscous-cutoff scale is not much smaller than that of the outer scale. Therefore, the exponential growth stage lasts for a long time until the magnetic energy density becomes comparable to the kinetic energy density at the outer scale of turbulence. In other words, the system is in exponential growth stage most of the time in high magnetic Prandtl number turbulence<sup>3</sup>.

During the exponential growth stage, the magnetic energy density follows

$$B^2(t) \propto B_0^2 \exp(t/\tau_d), \quad (2)$$

where  $B_0$  is the strength of the mean magnetic field and  $\tau_d$  is proportional to the eddy turnover time at the viscous-cutoff scale:  $\tau_d \propto l_d/v_d$ . The duration of the exponential growth stage is

$$t \propto \tau_d \ln(v_d^2/B_0^2) \propto (L/v) Re^{-1/2} \ln(v^2 Re^{-1/2}/B_0^2), \quad (3)$$

where we use  $v_l \propto l^{1/3}$  and  $L/l_d \sim Re^{3/4}$ . For a fixed  $Re$ , we get

$$t \propto C_1 - C_2 \ln B_0, \quad (4)$$

where  $C_1$  and  $C_2$  are constants that depend on  $Re$ . It is obvious from this equation that a weaker seed magnetic field takes more time to reach saturation. Therefore, if a seed magnetic field is so weak that the exponential growth stage takes more than the Hubble time, it cannot be the origin of cosmic magnetic fields.

If  $Re \sim O(1)$ , we get

$$t \sim (L/v) \ln B_{eq}^2/B_0^2, \quad (5)$$

<sup>2</sup> In this paper, by a high magnetic Prandtl number, we mean the hydrodynamic Reynolds number is less than  $\sim O(10^2)$  and the magnetic Reynolds number is much larger than the hydrodynamic Reynolds number.

<sup>3</sup> There might be a short linear growth stage after the exponential stage (see Cho & Yoo 2012). But, existence of the linear growth stage is not important in our current discussions.

where  $B_{eq}$  is the equipartition magnetic field (i.e.  $B_{eq}^2/4\pi = \rho v^2$ ), which is of order  $10^{-5}$  G in typical clusters. In this case, a seed magnetic field whose strength is weaker than

$$B_{0,crit} \sim B_{eq} \exp(-t_H v/2L), \quad (6)$$

where  $t_H$  is the age of the universe, cannot explain present-day magnetic fields in the ICM. In a cluster with  $L/v \sim 10^9$  years and  $B_{eq} \sim 10 \mu\text{G}$ , the critical strength would be

$$B_{0,crit} \sim 0.1 \mu\text{G}. \quad (7)$$

Note, however, that this estimate is highly uncertain because we ignored constants of order unity in many places while deriving Equation (5). In actual ICM, it is more complicated to obtain  $B_{0,crit}$  because  $Re$  can be greater than  $O(1)$ . Therefore, we need numerical simulations to get better estimates for  $B_{0,crit}$ .

### 3. NUMERICAL METHODS

#### 3.1. Numerical code

We use a pseudospectral code to solve the incompressible magnetohydrodynamic (MHD) equations in a periodic box of size  $2\pi$  ( $\equiv L_{sys}$ ):

$$\frac{\partial \mathbf{v}}{\partial t} = (\nabla \times \mathbf{B}) \times \mathbf{B} - (\nabla \times \mathbf{v}) \times \mathbf{v} + \nu \nabla^2 \mathbf{v} + \mathbf{f} + \nabla P', \quad (8)$$

$$\frac{\partial \mathbf{B}}{\partial t} = \nabla \times (\mathbf{v} \times \mathbf{B}) + \eta \nabla^2 \mathbf{B}, \quad (9)$$

where  $\nabla \cdot \mathbf{v} = \nabla \cdot \mathbf{B} = 0$ ,  $\mathbf{f}$  is random driving force,  $P' \equiv P + v^2/2$ ,  $\mathbf{v}$  is the velocity, and  $\mathbf{B}$  is the magnetic field divided by  $(4\pi\rho)^{1/2}$ . We use 22 forcing components in the wavenumber range  $2 < k < \sqrt{12}$ , which means the driving scale  $L$  is  $\sim L_{sys}/2.5$ . In our simulations,  $v \sim 1$  before saturation. Therefore, the large-scale eddy turnover time,  $\sim L/v$ , is approximately  $\sim 2.5$  before saturation. Other variables have their usual meaning. We use  $512^3$  grid points.

We use normal viscosity for the velocity dissipation term,  $\nu \nabla^2 \mathbf{v}$ , and hyperdiffusion for the magnetic dissipation term. The power of hyperdiffusion is set to 3, such that the magnetic dissipation term in Equation (9) is replaced with  $\eta_3 (\nabla^2)^3 \mathbf{B}$ . Therefore, the magnetic Prandtl number ( $= \nu/\eta$ ) is larger than one. Since we use hyperdiffusion, dissipation of magnetic field is negligible for small wavenumbers and it abruptly increases near  $(2/3)k_{max}$ , where  $k_{max}=256$ .

#### 3.2. Initial conditions

At  $t = 0$ , turbulence is fully developed and either a uniform or a localized seed magnetic field gets “switched on”. For localized seed magnetic fields, we consider two shapes: tube-like and doughnut-like seed magnetic fields.

For tube-shaped seed magnetic fields, we use the following expression for the magnetic field at  $t=0$ :

$$\mathbf{B}(r_\perp) = B_{max} e^{-r_\perp^2/2\sigma_0^2} \hat{\mathbf{x}}, \quad (10)$$

where  $\sigma_0 = 8$ ,  $r_\perp = (\Delta y^2 + \Delta z^2)^{1/2}$ , and  $\Delta y$  and  $\Delta z$  are the distances measured from the tube in grid units. The unit vector  $\hat{\mathbf{x}}$  is parallel to the x-axis. The maximum strength of the magnetic field at  $t=0$  is  $B_{max}$ .

For doughnut-shaped seed magnetic fields, we use the following expression for the magnetic field at  $t=0$ :

$$\mathbf{B}(\Delta x, r_\perp) = \frac{B_{max}}{2\sigma_0^2 e^{-1}} r_\perp^2 e^{-r_\perp^2/2\sigma_0^2} e^{-\Delta x^2/8\sigma_0^2} \hat{\theta}_\perp, \quad (11)$$

where  $B_{max} = 0.01$ ,  $\sigma_0 = 4\sqrt{2}$ ,  $r_\perp = (\Delta y^2 + \Delta z^2)^{1/2}$ , and  $\Delta x, \Delta y$ , and  $\Delta z$  are distances measured from the center of the numerical box in grid units. The unit vector  $\hat{\theta}_\perp$  is perpendicular to  $(\Delta x, 0, 0)$  and  $(0, \Delta y, \Delta z)$ . The maximum strength of the magnetic field at  $t=0$  is  $B_{max}$ . Since  $\sigma_0 = 4\sqrt{2}$  in Equation (11), the size of the magnetized region at  $t=0$  is  $\sim 16$  in grid units, which is  $\sim 1/32$  of the simulation box size. Therefore, in a cluster of size  $\sim 1$  Mpc, the size of the initially magnetized region corresponds to  $\sim 30$  kpc.

## 4. RESULTS

### 4.1. Results for uniform seed magnetic fields

Figure 1 shows the time evolution of  $B^2$  and  $v^2$ . In the simulations (Runs 512-R1-U's in Table 1), the viscosity is 0.015 and the driving scale is  $L = L_{sys}/k_f \sim 2.5$  and the velocity before saturation is  $\sim \sqrt{0.9}$ . Therefore, the hydrodynamic Reynolds number  $Re$  based on the velocity before saturation is roughly 160. Both the upper and the lower panels of Figure 1 show the time evolution of the same quantities, but the scales for the vertical axes are different; linear in the former and logarithmic in the latter. Initially only the uniform component of the magnetic field exists and, as time goes on, turbulent motions stretch magnetic field lines and make the magnetic field grow. As the magnetic energy density increases, the kinetic energy density of turbulence decreases. During the saturation stage, magnetic energy density is a bit higher than the kinetic energy density in all runs.

In Figure 1 we can clearly see that the exponential growth stage takes up most of the growth time (see the lower panel). It is possible that the exponential growth stage is followed by a linear growth stage (see discussions in Cho & Yoo 2012). However, because our  $Re$  is too small and, therefore, we do not fully resolve the inertial range, the duration of the linear growth stage, if any, should be very short.

In Figure 1, we can see that a weaker seed magnetic field takes more time to reach the saturation stage. When the maximum strength of the seed magnetic field is  $10^{-2}$ , which means that the maximum strength of the initial magnetic field is roughly  $10^{-2}$  times the equipartition magnetic field strength, the system reaches saturation within  $t \sim 5(L/v)$ . However, if the maximum strength of the seed magnetic field is  $10^{-6}$ , the system reaches saturation within  $t \sim 20(L/v)$ .

Consider a cluster with  $L \sim 400$  kpc,  $v \sim 400$  km/s and equipartition magnetic field of  $\sim 10 \mu\text{G}$ . In this case, the large-scale eddy turnover time is

$$L/v \sim 10^9 \text{ years}. \quad (12)$$

If the strength of the initial seed magnetic field is  $0.01$  nG, which is  $10^{-6}$  times the equipartition magnetic field strength, the system reaches saturation  $\sim 20$  billion years after the big bang. This simple argument implies that any primordial seed magnetic field weaker than  $\sim 0.01$  nG cannot be the direct origin of cosmic magnetism. Note

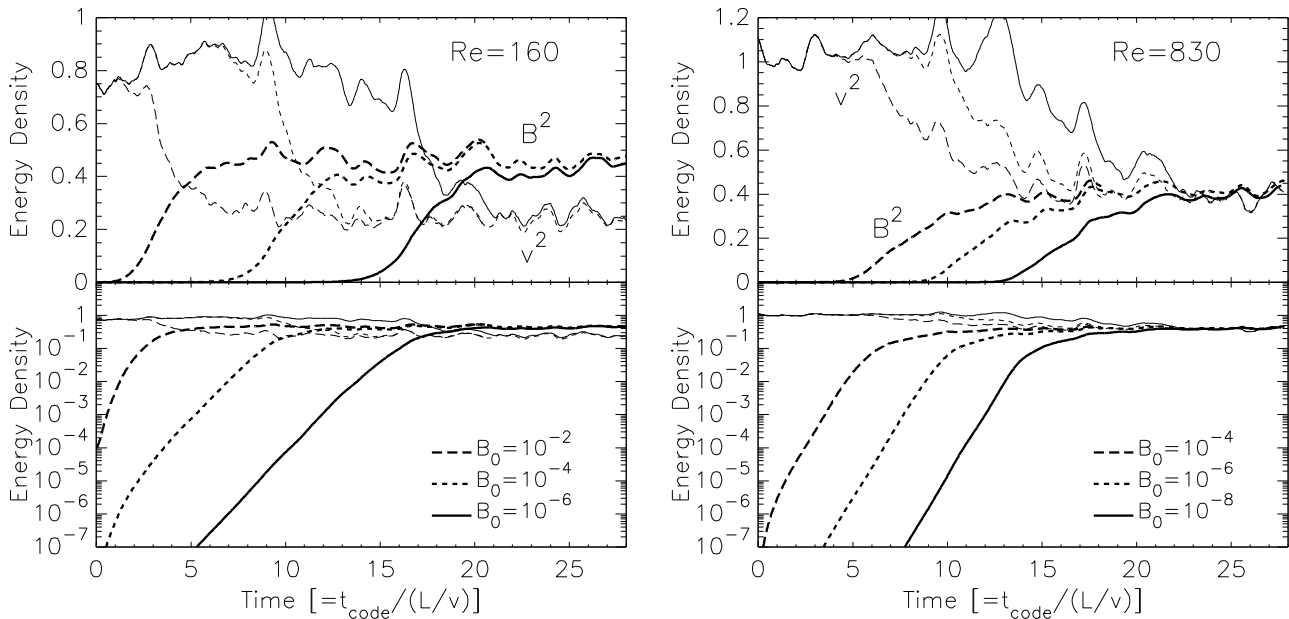


**Figure 1.** Growth of uniform seed magnetic fields in a high magnetic Prandtl number turbulence with the hydrodynamic Reynolds number ( $Re$ ) of  $\sim 160$ . The scales for the vertical axes are different: linear in the upper panel and logarithmic in the lower panel. The exponential growth stage takes up most of the growth time. The growth time of  $B^2$  depends on the strength of the uniform seed field,  $B_0$ : a weaker seed field reaches the saturation stage later. From Runs 512-R1-UB $010^{-2}$ , 512-R1-UB $010^{-4}$ , and 512-R1-UB $010^{-6}$ .

**Figure 2.** Growth of uniform seed magnetic fields in a high magnetic Prandtl number turbulence with  $Re \sim 830$ . It seems that the exponential growth stage is followed by a short linear growth stage. Although the growth time of  $B^2$  depends on the strength of the uniform seed magnetic field,  $B_0$ , the dependence is less pronounced compared with the results in Figure 1. From Runs 512-R2-UB $010^{-4}$ , 512-R2-UB $010^{-6}$ , and 512-R2-UB $010^{-8}$ .

that the large-scale eddy turnover time in Equation (12) is in rough agreement with the values in some numerical simulations of the large-scale structure formation (see, for example, Ryu et al. 2008).

As aforementioned, we expect that  $Re \lesssim 10^2$  in the ICM (see Equation (1)). Nevertheless, it could be possible that  $Re > 10^2$  in some clusters. Therefore, it is worth investigating turbulence dynamo for a higher  $Re$ . In Figure 2 we present results of simulations for a higher  $Re$ . In the simulations (Runs 512-R2-U's in Table 1), the viscosity is 0.003, the driving scale is  $L = L_{sys}/k_f \sim 2.5$ , and the velocity before saturation is  $\sim 1.0$ , so that  $Re$  based on the velocity before saturation is roughly 830. As in Figure 1, we can clearly see the exponential growth stage and, now, we can see that a short, but clearly visible, linear growth stage follows the exponential growth stage. As in Figure 1, a weaker seed magnetic field takes more time to reach saturation. But now the growth rate of magnetic field is higher because the eddy turnover time at the viscous-cutoff scale is shorter. Therefore, compared with runs in Figure 1, somewhat weaker seed magnetic fields can be the direct origin of magnetic field in the ICM. Figure 2 shows that a seed magnetic field as weak as  $10^{-8}$  times the equipartition strength can reach saturation within  $\sim 20(L/v)$ . If we consider the same cluster as before, a seed magnetic field as weak as  $10^{-4}$  nG can reach saturation  $\sim 20$  billion years after the big bang.

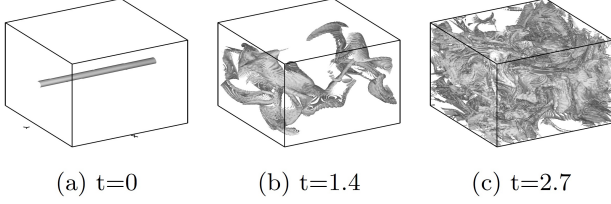
#### 4.2. Results for localized seed magnetic fields

In this subsection, we investigate how localized seed magnetic fields grow in high magnetic Prandtl number

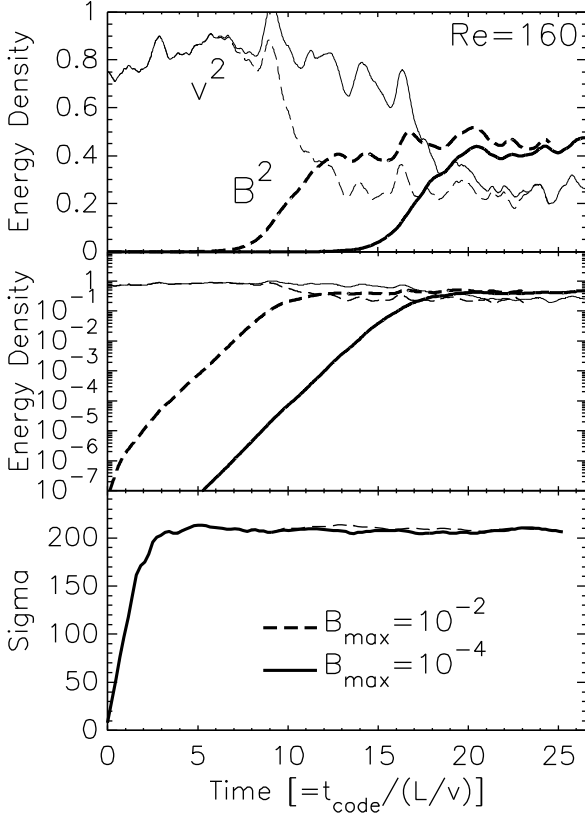
turbulence. In all simulations in this subsection (Runs 512-R1-T's and 512-R1-D's in Table 1), the viscosity is 0.015 and the driving scale is  $L = L_{sys}/k_f \sim 2.5$  and the velocity before saturation is  $\sim \sqrt{0.9}$ , so that  $Re$  based on the velocity before saturation is roughly 160. If the seed magnetic field is localized in space, turbulent motions stretch and disperse magnetic field lines, which makes the magnetic field grow and, at the same time, the magnetized region expand in high magnetic Prandtl number turbulence as in unit magnetic Prandtl number turbulence.

Figure 3 shows that the homogenization of a tube-shaped seed magnetic field is very fast. The figure shows that the whole numerical box becomes magnetized within  $\sim 2.7(L/v)$  (see more quantitative results in the lower panel of Figure 4). In our simulations, the size of the computational box is  $\sim 2.5L$ . Therefore, the observed rate of homogenization implies that the speed at which the magnetized region expands is of order  $v$  in high magnetic Prandtl number turbulence as in unit magnetic Prandtl number turbulence.

Figure 4 shows the time evolution of  $B^2$ ,  $v^2$ , and the standard deviation of the magnetic field distribution, which can be regarded as an approximate size of the magnetized region. Both the upper and the middle panels of Figure 4 show the time evolution of  $B^2$  and  $v^2$ , but the scales for the vertical axes are different. Initially only the localized seed magnetic field exists and, as time goes on, turbulent motions make the magnetic field grow. As the magnetic energy density increases, the kinetic energy density of turbulence decreases. The values of  $B^2$  and  $v^2$  at the saturation stage are very similar to those for uni-



**Figure 3.** Homogenization of a tube-shaped localized seed magnetic field in high magnetic Prandtl number turbulence. The expansion of the magnetized region happens very fast. After homogenization, the subsequent evolution should be very similar to that of a uniform seed magnetic field case. The driving scale is about 2.5 times smaller than the size of the computational box. In the shaded regions, the magnetic field is stronger than 0.1 times  $B_{max}$ . From Run 512-R1-TB $B_{max}10^{-2}$ .



**Figure 4.** Growth of tube-shaped localized seed magnetic fields in high magnetic Prandtl number turbulence. The upper and the middle panels show the time evolution of the same quantities,  $B^2$  and  $v^2$ , but their vertical scales are different: linear in the upper panel and logarithmic in the middle panel. The lower panel shows the time evolution of the standard deviation of the magnetic field distribution,  $\sigma$ . In the lower panel, the two curves for  $B_{max} = 10^{-2}$  and  $10^{-4}$  almost coincide. From Runs 512-R1-TB $B_{max}10^{-2}$  and 512-R1-TB $B_{max}10^{-4}$ .

form seed field cases (compare Figures 4 and 1).

In the lower panel of Figure 4, we plot the time evolution of the standard deviation,  $\sigma$ , of magnetic field distribution:

$$\sigma = (\sigma_y^2 + \sigma_z^2)^{1/2}, \quad (13)$$

$$\sigma_i^2 = \frac{\int (x_i - \bar{x}_i)^2 |\mathbf{B}(\mathbf{x}, t)|^2 d^3x}{\int |\mathbf{B}(\mathbf{x}, t)|^2 d^3x}, \quad (14)$$

$$\bar{x}_i = \frac{\int x_i |\mathbf{B}(\mathbf{x}, t)|^2 d^3x}{\int |\mathbf{B}(\mathbf{x}, t)|^2 d^3x}, \quad (15)$$

where  $i=y$  and  $z$ . Initially the standard deviation rises very quickly and the growth rate decreases after  $\sim 1.5(L/v)$ . Within  $\sim 3(L/v)$ , the standard deviation almost reaches the value for homogeneous distribution. The behavior of  $\sigma$  is not sensitive to the value of  $B_{max}$ : in fact, the curves for  $B_{max}10^{-2}$  and  $B_{max}10^{-4}$  virtually coincide.

Since the seed magnetic field in Run 512-R1-TB $B_{max}10^{-2}$  (dashed curve) is stronger than that in Run 512-R1-TB $B_{max}10^{-4}$  (solid curve), Run 512-R1-TB $B_{max}10^{-2}$  reaches saturation earlier. Note that Run 512-R1-TB $B_{max}10^{-4}$  reaches saturation within  $\sim 20(L/v)$ . Therefore, for a cluster of galaxies with  $L/v \sim 10^9$  years, any tube-like seed magnetic field weaker than  $\sim 10^{-4}$  times the equipartition strength cannot produce a strong enough magnetic field within the Hubble time. For example, if we consider the same cluster as before ( $L_{sys}=1$  Mpc,  $L=400$  kpc,  $v \sim 400$  km/s,  $Re = 160$ , and the equipartition magnetic field strength of  $\sim 10\mu\text{G}$ ), it is likely that any localized tube-shaped seed magnetic field that is weaker than  $\sim 1$  nG cannot be the origin of magnetic field in the ICM. Of course, if  $Re$  is larger, the minimum magnetic field strength will decrease.

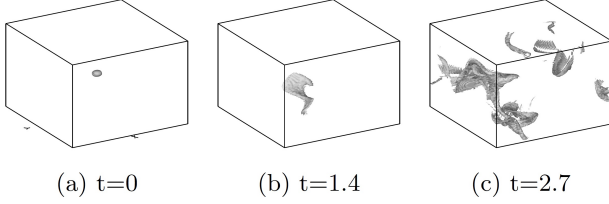
Figure 5 shows that the homogenization time for a doughnut-shaped seed magnetic field is also very fast. The figure shows that the magnetic field spreads out and fills the whole numerical box within  $\sim 2.7(L/v)$ . Actually, if we plot the time evolution of the standard deviation,  $\sigma$ , of magnetic field distribution,

$$\sigma = (\sigma_x^2 + \sigma_y^2 + \sigma_z^2)^{1/2}, \quad (16)$$

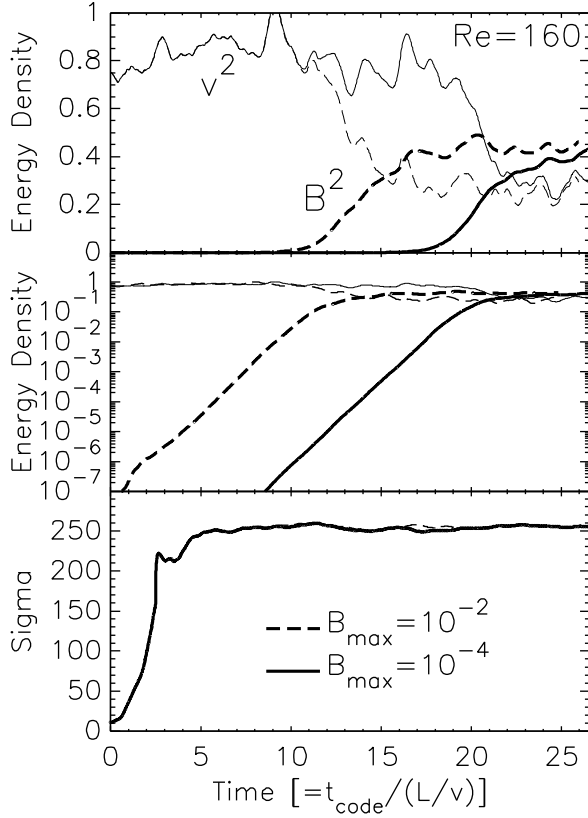
where  $\sigma_i^2$ ,  $i=x, y$ , and  $z$ , is defined as in Equation (14), it reaches the value for homogeneous distribution after  $\sim 4(L/v)$  (the lower panel of Figure 6). As in the tube-like seed magnetic field cases, the behavior of  $\sigma$  is not sensitive to the value of  $B_{max}$ : the curves for  $B_{max}10^{-2}$  and  $B_{max}10^{-4}$  almost coincide. As we discussed above, the observed rate of homogenization is consistent with the fact that the speed at which the magnetized region expands is of order  $v$ . If we compare homogenization of a tube-like seed magnetic field (Figure 3) and a doughnut-like seed magnetic field (Figure 5), the latter produces more intermittent magnetic field distribution during and at the end of the homogenization process.

Figure 6 shows the time evolution of  $B^2$ ,  $v^2$ , and  $\sigma$ . The Run 512-R1-DB $B_{max}10^{-2}$  reaches saturation after  $\sim 15(L/v)$  and the Run 512-R1-DB $B_{max}10^{-4}$  reaches saturation after  $\sim 25(L/v)$ . Therefore, for a cluster of galaxies with  $L/v \sim 10^9$  years, any doughnut-like seed magnetic field weaker than  $\sim 10^{-3}$  times the equipartition strength cannot produce a strong enough magnetic field within the Hubble time. For example, if we consider the cluster of galaxies mentioned earlier ( $L_{sys}=1$  Mpc,  $L=400$  kpc,  $v \sim 400$  km/s,  $Re = 160$ , and equipartition magnetic field strength of  $\sim 10\mu\text{G}$ ), it is likely that any localized doughnut-shaped seed magnetic field whose maximum strength is weaker than  $\sim 10\text{nG}$  cannot be the origin of magnetic field in the ICM.

## 5. DISCUSSIONS



**Figure 5.** Homogenization of a doughnut-shaped localized seed magnetic field in high magnetic Prandtl number turbulence. The expansion of the magnetized region happens very fast. After homogenization, the subsequent evolution should be very similar to that of a uniform seed magnetic field case. The driving scale is about 2.5 times smaller than the size of the computational box. In the shaded regions, the magnetic field is stronger than 0.1 times  $B_{\max}$ . From Run 512-R1-DB $_{\max}10^{-2}$ .



**Figure 6.** Growth of doughnut-shaped localized seed magnetic fields in high magnetic Prandtl number turbulence. The upper and the middle panels show the time evolution of the same quantities,  $B^2$  and  $v^2$ . The lower panel shows the time evolution of the standard deviation of the magnetic field distribution  $\sigma$ . In the lower panel, the two curves for  $B_{\max} = 10^{-2}$  and  $10^{-4}$  almost coincide. From Runs 512-R1-DB $_{\max}10^{-2}$  and 512-R1-DB $_{\max}10^{-4}$ .

### 5.1. Primordial or Astrophysical?

Our simulations show that the strength of a uniform seed magnetic field should be larger than  $O(10^{-11})\text{G}$  if  $Re \sim 160$  in the ICM<sup>4</sup>. Note that observations of the Cosmic Microwave Background (CMB) place an upper limit

<sup>4</sup> In case  $Re$  is smaller than 160, the minimum strength of the seed magnetic field will be larger than  $O(10^{-11})\text{G}$ . If  $Re \sim 28$  as in Equation (1), we expect that the minimum strength will be at least  $O(10^{-10})\text{G}$ .

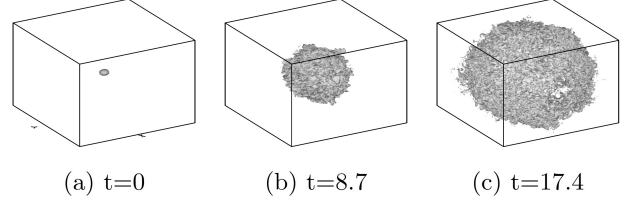


**Figure 7.** Same as Figure 5, but the driving scale is smaller: it is about 20 times smaller than a side of the computational box. From Run 512-REF.

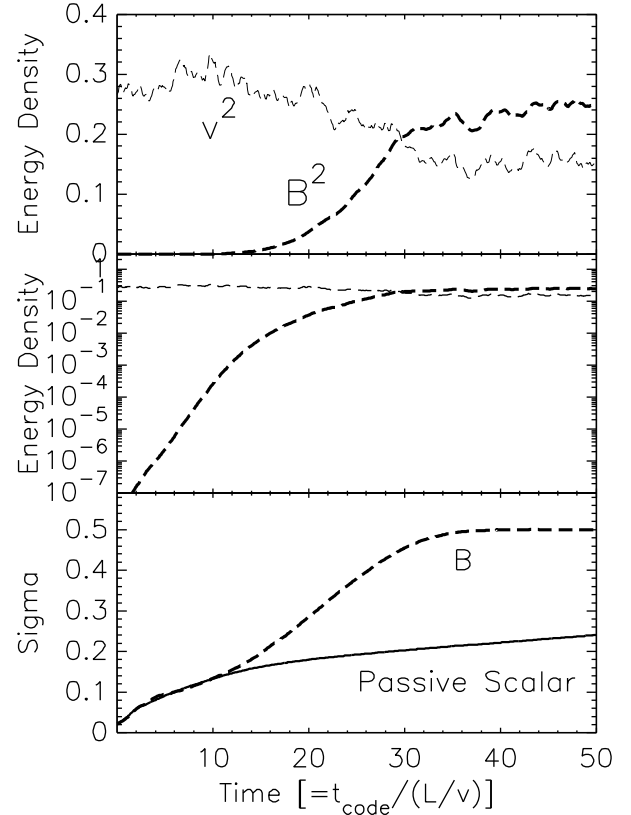


**Figure 8.** Growth of doughnut-shaped localized seed magnetic fields in high magnetic Prandtl number turbulence with a small-scale driving: the driving scale is about 20 times smaller than a side of the computational box. The upper and the middle panels show the time evolution of the same quantities,  $B^2$  and  $v^2$ . The lower panel shows the time evolution of the standard deviation of the magnetic field (the dashed line) and the passive scalar field (the solid line) distributions. From Run 512-REF.

of  $O(10^{-9})\text{G}$  on the strength of the uniform component of a primordial seed magnetic field (Barrow, Ferreira & Silk 1997; see also Widrow et al. 2012; Durrer & Neronov 2013). Therefore, it is unlikely that primordial magnetic fields are the direct origin of present-day magnetic fields in the ICM.

If the high magnetic Prandtl number model is correct for fluids in the ICM, it is also unlikely that a magnetic field generated by the Biermann battery ( $B \sim 10^{-20}\text{G}$ ) or aperiodic turbulent fluctuations (Schlickheiser 2012;  $B \sim 10^{-16}\text{G}$ ) are the direct source of magnetic fields in the ICM. However, it is still possible that pre-galactic magnetic fields generated by the battery effect or the aperiodic turbulent fluctuations became amplified in galax-

ies (see Kulsrud & Zweibel 2008 and references therein; see also discussions in Beck & Wielebinski 2013) or first stars (Sur et al. 2010; Schleicher et al. 2010; Schober et al. 2012b; Schleicher et al. 2013) and then ejected into the intergalactic space later. Such ejected magnetic fields can easily be the origin of cosmic magnetic fields even in high magnetic Prandtl number turbulence. All in all, our simulations favor astrophysical origin of the ICM magnetic fields.

### 5.2. Homogenization rate

Cho & Yoo (2012) showed that expansion of the magnetized region is fast in unit magnetic Prandtl number turbulence: homogenization of a doughnut-shaped seed magnetic field in unit magnetic Prandtl number turbulence occurs within  $\sim 3(L/v)$ . The numerical setup in Cho & Yoo (2012) is almost identical to our current numerical setup for the doughnut-shaped seed magnetic fields, excepts the magnetic Prandtl numbers (i.e. the values of the viscosity). Our current simulations show that expansion of magnetized region is also fast in high Prandtl number turbulence: homogenization of a tube-like seed field occurs within  $\sim 3(L/v)$  and homogenization of a doughnut-like seed field occurs within  $\sim 4(L/v)$ . In our current simulations, the large viscosity damps small-scale velocity. Nevertheless, we obtain fast homogenization in our current simulations. Why is it so? It seems that expansion of the magnetized region is governed by eddy motions at the outer scale of turbulence. Inside an outer-scale eddy, magnetization of the whole eddy happens roughly within one large-scale eddy turnover time if the size of the initially magnetized region is not much smaller than the viscous-cutoff scale. After full magnetization of the outer-scale eddy, the magnetic field is transported over uncorrelated outer-scale eddies. Because any outer-scale eddy which is partially magnetized can be fully magnetized within roughly one large-scale eddy turnover time, the rate of expansion of the magnetized region should be proportional to  $v$  (Cho 2013). Therefore, full magnetization of the system occurs within  $\sim L_{sys}/v$ , which we actually observe in our simulations.

Can we numerically confirm that the expansion speed of the magnetized region is indeed of order  $v$  in high magnetic Prandtl number turbulence? To measure the expansion rate on scales larger than the outer-scale eddies, we perform a numerical simulation with a small-scale driving (512-REF in Table 1). Simulation setup for 512-REF is identical to that for 512-R1-DB $_{max}10^{-4}$  except the the driving scale: the driving wave-numbers for 512-REF are between 15.4 and 26. The hydrodynamic Reynolds number  $Re$  for 512-REF is an order of magnitude smaller than that for 512-R1-DB $_{max}10^{-4}$  because the driving scale for 512-REF is an order of magnitude smaller. We plot the simulation results in Figures 7 and 8. Figure 7 shows the expansion of the magnetized region and Figure 8 shows the time evolution of  $B^2$ ,  $v^2$ , and the standard deviations. If we compare the rates of expansion for  $0 \leq t \leq 8.7$  and for  $8.7 \leq t \leq 17.4$  in Figure 7, the rates look similar, which implies that the expansion rate is linear in time. Indeed the lower panel of Figure 8 shows that the standard deviation of magnetic field distribution (the dashed curve; see Equation (16) for definition) shows a linear growth after a certain time,

before which its behavior is very similar to that of a passive scalar field (the solid curve). This behavior is very similar to that of a localized seed magnetic field in unit magnetic Prandtl number turbulence (see Cho 2013 for numerical methods and detailed discussions).

### 5.3. Discussions on the localized seed magnetic fields

If the initially magnetized region is smaller than the viscous-cutoff scale  $l_d \sim Re^{-3/4}L$ , the expansion speed of the magnetized region can be slower than  $\sim v$ . Let the size of the initially magnetized region be  $D_s$ . If  $D_s < l_d$ , then it takes

$$\sim \frac{l_d}{v_d} \left( \frac{l_d}{D_s} \right)^2 \sim Re^{-2} \left( \frac{L}{D_s} \right)^2 \left( \frac{L}{v} \right) \quad (17)$$

for the magnetic field to fill the ‘host’ eddy at the viscous-cutoff scale. After filling the viscous-cutoff-scale eddy, it would take  $\sim L/v$  for the magnetic field to fill the whole outer-scale eddy. Therefore, in this case, magnetization of the outer-scale eddy takes

$$\sim (1 + Re^{-2}(L/D_s)^2) \left( \frac{L}{v} \right). \quad (18)$$

The expansion rate of the magnetized region on scales larger than the outer scale of turbulence will be

$$\sim v / (1 + Re^{-2}(L/D_s)^2) \quad (19)$$

For a cluster with  $L \sim 400$  kpc and  $D_s \sim 30$  kpc, we will have  $D_s < l_s$  if  $Re < (L/D_s)^{4/3} \sim 30$ . But, for this  $Re$ , slowdown of the expansion rate will be negligible (see Equation (19)). Slowdown of the expansion rate will be important when  $Re < (L/D_s) \sim 13$  in the cluster. Note, however, that, if the magnetized materials in jets or stripped gases provide seeding, the initially magnetized region can be up to hundreds-of-kpc-long and, therefore,  $Re$  can be smaller than this.

In the ISM of galaxies, strength of the magnetic fields ranges from  $\sim \mu\text{G}$  (diffuse ISM) to  $\sim \text{mG}$  (molecular clouds). When these gases are expelled from galaxies, magnetic fields in them will be attenuated due to expansion of the media. This makes the strength of the localized seed magnetic fields weaker than the galactic values. If a linear size of the medium expands by a factor of  $f_e$  during the ejection, magnetic field becomes weaker by a factor of  $f_e^{-2}$ . The magnetic attenuation factor  $f_e^{-2}$  is uncertain and may depend on the ejection mechanism. If a galactic material is ejected via jets or explosions, the expansion factor can be very large. For example, if a jet is launched from a sub-pc scale and ultimately expands to kpc-scales, the expansion factor can be larger than  $10^3$  (see related discussions in Brandenburg & Subramanian 2005; Widrow et al. 2012). However, if a magnetized gas is stripped from a galaxy, the expansion factor can be smaller than  $10^3$ . Another factor that can affect the strength of the seed fields is existence of turbulence inside ejecta. If turbulence exists inside the ejected media, turbulence dynamo can mitigate attenuation of the magnetic fields.

### 5.4. Observational implications



If we use the turbulence dynamo models, we can test whether or not the high magnetic Prandtl number turbulence is a correct model for the ICM or the intergalactic medium. Suppose that we can observe distribution of magnetic fields in filaments. If distribution of magnetic fields in filaments is more or less homogeneous, it is likely that the high magnetic Prandtl number turbulence model is incorrect. If we find magnetic fields only near the astrophysical sources, we may be able to conclude that magnetic fields in filaments have astrophysical origins, rather than primordial.

### 5.5. Effects of compression

The use of an incompressible code has the advantage that we can easily control the viscosity and the magnetic diffusivity. However, it is not possible to study the effects of compression with the incompressible code. In galaxy clusters, shocks and mergers can compress fluids and have a pronounced impact on the growth of magnetic field (Roettiger et al 1999; Dolag et al. 1999, 2002; Iapichino & Brüggén 2012). For example, a simulation by Dolag et al. (2002) shows that the mean magnetic field within a cluster of comoving radius 1 Mpc increases by a factor of  $\sim 30$  from redshift  $z=0.8$  to  $z=0$ . If this is a typical growth factor for compression amplification, the minimum strength of a uniform magnetic field for  $Re=160$  should be decreased by the same factor: a new minimum strength will be a few times  $10^{-13}G$ . Note, however, that  $Re$  in actual clusters is likely to be much smaller than 160 (see Equation (1)). Therefore, if we take into account both the compression amplification and a realistic  $Re$ , the minimum strength may not be much smaller than  $O(10^{-11})G$ .

It is likely that the central region of a galaxy cluster has formed at a much earlier stage. During these early stages, many of the physical properties, including the hydrodynamic Reynolds number  $Re$ , could be different. It is therefore conceivable that some magnetization has occurred already at earlier stages, which can alleviate the constraints found in this paper. However, unless such central regions were substantially cooler and/or denser than present-day central regions, the effect may not be significant. Note that, even in present-day cool cores,  $Re$  is expected to be less than  $\sim 10^2$  (Schekochihin & Cowley 2006).

## 6. SUMMARY

In this paper, we have considered turbulence dynamo models in unit and high magnetic Prandtl number fluids. We have found the following results:

1. In high magnetic Prandtl number turbulence (with a hydrodynamic Reynolds number,  $Re$ , less than  $O(10^2)$ ), turbulence dynamo is not so efficient that a primordial seed magnetic field weaker than a certain critical value cannot be a direct origin of magnetic fields in the ICM. For a cluster with driving scale of  $\sim 400$  kpc and turbulence velocity of  $\sim 400$  km/s, the critical strength is  $\sim 10^{-11}G$  for  $Re = 160$ , which is very close to an upper limit of  $O(10^{-9})G$  placed by the CMB anisotropy observations. The critical strengths for seed magnetic fields ejected from galaxies or first stars are about two orders of magnitude higher. But, since

the strengths of magnetic fields in those astrophysical objects are likely to be larger than  $\mu G$ , it may not be so difficult for the seed magnetic fields ejected from the astrophysical bodies to have strengths larger than the critical values. Therefore, our calculations favor astrophysical origin of magnetic fields in the ICM.

2. If the high magnetic Prandtl number model is correct for clusters and filaments, pre-galactic magnetic fields generated by a battery effect, amplified in galaxies or first stars, and ejected from them later into intergalactic space would be plausible sources of magnetic fields in the large-scale structure of the universe.

We thank the referee for useful suggestions and comments. This work is supported by the National R & D Program through the National Research Foundation of Korea, funded by the Ministry of Education (NRF-2013R1A1A2064475). This work is also supported by the Supercomputing Center/Korea Institute of Science and Technology Information with supercomputing resources including technical supports (KSC-2013-C1-034).

## REFERENCES

- Arieli, Y., Rephaeli, Y., & Norman, M. L. 2011, *ApJ*, 738, 15  
 Banerjee, R., & Jedamzik, K. 2004, *Phys. Rev. D*, 70, 123003  
 Barrow, J., Ferreira, P., & Silk, J. 1997, *Phys. Rev. Lett.*, 78, 3616  
 Batchelor, G. 1950, *Proc. R. Soc. London A*, 201, 405  
 Beck, R., & Wielebinski, R. 2013, *Planets, Stars and Stellar Systems. Volume 5: Galactic Structure and Stellar Populations*, 641  
 Beresnyak, A. 2012, *Phys. Scr*, 86, 058201  
 Biermann, L. 1950, *Zeitschrift Naturforschung Teil A*, 5, 65  
 Bovino, S., Schleicher, D. R. G., & Schober, J. 2013, *New Journal of Physics*, 15, 013055  
 Brandenburg, A., Sokoloff, D., & Subramanian, K. 2012, *Space Sci. Rev.*, 169, 123  
 Brandenburg, A., & Subramanian, K. 2005, *Phys. Reports*, 417, 1  
 Brunetti, G., & Lazarian, A. 2007, *MNRAS*, 378, 245  
 Carilli, C. L., & Taylor, G. B. 2002, *ARA&A*, 40, 319  
 Childress, S., & Gilbert, A. 1995, *Stretch, Twist, Fold: The Fast Dynamo* (Berlin: Springer)  
 Cho, J. 2013, *Phys. Rev. D*, 87, 043008  
 Cho, J., & Vishniac, E. T. 2000, *ApJ*, 538, 217  
 Cho, J., Vishniac, E. T., Beresnyak, A., Lazarian, A., & Ryu, D. 2009, *ApJ*, 693, 1449  
 Cho, J., & Yoo, H. 2012, *ApJ*, 759, 91  
 Daly, R. A., & Loeb, A. 1990, *ApJ*, 364, 451  
 Donnert, J., Dolag, K., Lesch, H., Müller, E. 2009, *MNRAS*, 392, 1008  
 Dolag, K., Bartelmann, M., & Lesch, H. 1999, *A&A*, 348, 351  
 Dolag, K., Bartelmann, M., & Lesch, H. 2002, *A&A*, 387, 383  
 Durrer, R., & Neronov, A. 2013, *A&A Rev.*, 21, 62  
 Ferrari, C., Govoni, F., Schindler, S., Bykov, A. M., & Rephaeli, Y. 2008, *Space Sci. Rev.*, 134, 93  
 Haugen, N. E., Brandenburg, A., & Dobler, W. 2004, *Phys. Rev. E*, 70, 016308  
 Hoyle, F. 1969, *Nature*, 223, 936  
 Iapichino, L., & Brüggén, M. 2012, *MNRAS*, 423, 2781  
 Govoni, F., & Feretti, L. 2004, *International Journal of Modern Physics D*, 13, 1549  
 Kazantsev, A. P. 1968, *Soviet Phys.-JETP Lett.*, 26, 1031  
 Kronberg, P. P. 1994, *Reports on Progress in Physics*, 57, 325  
 Kronberg, P. P., Dufton, Q. W., Li, H., & Colgate, S. A. 2001, *ApJ*, 560, 178  
 Kulsrud, R. M., & Anderson, S. W. 1992, *ApJ*, 396, 606



**Table 1**  
Simulations.

Run	Resolution	Reynolds No.	$B_{max}$ at $t=0^a$	$B_0^b$	$Pr_m^c$	Seed Field	$L_{sys}/L^d$
512-R1-UB $_0 10^{-2}$	512 <sup>3</sup>	$\sim 160$	-	$10^{-2}$	high	uniform	$\sim 2.5$
512-R1-UB $_0 10^{-4}$	512 <sup>3</sup>	$\sim 160$	-	$10^{-4}$	high	uniform	$\sim 2.5$
512-R1-UB $_0 10^{-6}$	512 <sup>3</sup>	$\sim 160$	-	$10^{-6}$	high	uniform	$\sim 2.5$
512-R2-UB $_0 10^{-4}$	512 <sup>3</sup>	$\sim 830$	-	$10^{-4}$	high	uniform	$\sim 2.5$
512-R2-UB $_0 10^{-6}$	512 <sup>3</sup>	$\sim 830$	-	$10^{-6}$	high	uniform	$\sim 2.5$
512-R2-UB $_0 10^{-8}$	512 <sup>3</sup>	$\sim 830$	-	$10^{-8}$	high	uniform	$\sim 2.5$
512-R1-TB $_{max} 10^{-2}$	512 <sup>3</sup>	$\sim 160$	$10^{-2}$	-	high	tube-shaped	$\sim 2.5$
512-R1-TB $_{max} 10^{-4}$	512 <sup>3</sup>	$\sim 160$	$10^{-4}$	-	high	tube-shaped	$\sim 2.5$
512-R1-DB $_{max} 10^{-2}$	512 <sup>3</sup>	$\sim 160$	$10^{-2}$	-	high	doughnut-shaped	$\sim 2.5$
512-R1-DB $_{max} 10^{-4}$	512 <sup>3</sup>	$\sim 160$	$10^{-4}$	-	high	doughnut-shaped	$\sim 2.5$
512-REF	512 <sup>3</sup>	$\sim 10$	$10^{-4}$	-	high	doughnut-shaped	$\sim 20$

<sup>a</sup> Maximum strength of the localized magnetic field at  $t=0$ .<sup>b</sup> Strength of the uniform magnetic field.<sup>c</sup> Magnetic Prandtl number ( $\equiv \nu/\eta$ ).<sup>d</sup>  $L_{sys}$  is the system size and  $L$  is the driving scale.

Kulsrud, R. M., Cen, R., Ostriker, J. P., & Ryu, D. 1997, *ApJ*, 480, 481  
Kulsrud, R. M., & Zweibel, E. G. 2008 Reports on Progress in Physics, 71, 046901  
Meneguzzi, M., Frisch, U., & Pouquet, A. 1981, *Physical Review Letters*, 47, 1060  
Miniati, F. 2014, *ApJ*, 782, 21  
Molchanov, S., Ruzmaikin, A., & Sokolov, D. 1985, *Sov. Phys. Usp.*, 28, 307  
Pouquet, A., Frisch, U., & Leorat, J. 1976, *Journal of Fluid Mechanics*, 77, 321  
Pudritz, R. E., & Silk, J. 1989, *ApJ*, 342, 650  
Rephaeli, Y. 1988, *Comments on Astrophysics*, 12, 265  
Rees, M. J. 1987 *Royal Astronomical Society, Quarterly Journal*, 28, 197  
Reynolds, C., McKernan, B., Fabian, A., Stone, J., & Vignello, J. 2005, *MNRAS*, 357, 242  
Robinson, K., Dursi, L. J., Ricker, P. M., et al. 2004, *ApJ*, 601, 621  
Roettiger, K., Stone, J. M., & Burns, J. O. 1999, *ApJ*, 518, 594  
Ruszkowski, M., Brüggemann, M., & Begelman, M. 2004, *ApJ*, 611, 158  
Ruzmaikin, A., Sokoloff, D., & Shukurov, A. 1989, *MNRAS*, 241, 1  
Ryu, D., Kang, H., Cho, J., & Das, S. 2008, *Science*, 320, 909  
Ryu, D., Schleicher, D. R. G., Treumann, R. A., Tsagas, C. G., & Widrow, L. M. 2012, *Space Sci. Rev.*, 166, 1  
Schekochihin, A. A., & Cowley, S. C. 2006, *Physics of Plasmas*, 13, 056501  
Schekochihin, A., & Cowley, S. 2007, in *Magnetohydrodynamics - Historical evolution and trends*, eds. by Molokov, S., Moreau, R., & Moffatt, H. (Berlin; Springer), p. 85 (astro-ph/0507686)  
Schekochihin, A. A., Cowley, S. C., Taylor, S. F., Maron, J. L., & McWilliams, J. C. 2004, *ApJ*, 612, 276

Schleicher, D. R. G., Banerjee, R., Sur, S., et al. 2010, *A&A*, 522, A115  
Schleicher, D. R. G., Latif, M., Schober, J., et al. 2013, *Astronomische Nachrichten*, 334, 531  
Schlickeiser, R. 2012, *Physical Review Letters*, 109, 261101  
Schlüter, A., & Biermann, I. 1950, *Zeitschrift Naturforschung Teil A*, 5, 237  
Schober, J., Schleicher, D., Federrath, C., Klessen, R., & Banerjee, R. 2012a, *Phys. Rev. E*, 85, 026303  
Schober, J., Schleicher, D., Federrath, C., et al. 2012b, *ApJ*, 754, 99  
Spitzer, L. 1962, *Physics of Fully Ionized Gases* (New York: Wiley)  
Subramanian, K., Shukurov, A., & Haugen, N. 2006, *MNRAS*, 366, 1437  
Sur, S., Schleicher, D. R. G., Banerjee, R., Federrath, C., & Klessen, R. S. 2010, *ApJ*, 721, L134  
Vainshtein, S. I., & Ruzmaikin, A. A. 1972, *Soviet Ast.*, 15, 714  
Vazza, F., Brunetti, G., Gheller, C., Brunino, R., & Brüggemann, M. 2011, *A&A*, 529, A17  
Vogt, C., & Enßlin, T. A. 2005, *A&A*, 434, 67  
Wagstaff, J. M., Banerjee, R., Schleicher, D., & Sigl, G. 2014, *Phys. Rev. D*, 89, 103001  
Widrow, L. M. 2002, *Reviews of Modern Physics*, 74, 775  
Widrow, L. M., Ryu, D., Schleicher, D. R. G., et al. 2012, *Space Sci. Rev.*, 166, 37  
Xu, H., Li, H., Collins, D. C., Li, S., & Norman, M. L. 2010, *ApJ*, 725, 2152  
Yoo, H., & Cho, J. 2014, *ApJ*, 780, 99  
Zeldovich, Ya. B., Ruzmaikin, A. A., Molchanov, S. A., & Sokoloff, D. D. 1984, *J. Fluid Mech.*, 144, 1  
Zweibel, E. G., & Heiles, C. 1997, *Nature*, 385, 131

## APPENDIX

## TURBULENCE DYNAMO MODEL IN UNIT MAGNETIC PRANDTL NUMBER FLUIDS

In this Appendix, we briefly review turbulence dynamo models in unit magnetic Prandtl number turbulence and discuss their implications. We assume that the fluid is incompressible and that both the viscosity and the magnetic diffusivity are very small. When the magnetic Prandtl number is unity, the velocity and the magnetic dissipation scales coincide.

If a seed magnetic field has a primordial origin, the coherence length of the seed field can be very large and, therefore, it can be regarded as spatially uniform on the scale of galaxy clusters. Even if the primordial seed magnetic field has a small coherence length (see, for example, Banerjee & Jedamzik 2004; Wagstaff et al. 2014), turbulence dynamo for the seed field will be similar to that for a uniform seed field, as long as the seed field is spatially homogeneous. On the other hand, if a seed magnetic field was provided by an astrophysical object, it is likely that the seed magnetic field was spatially localized at the time of injection.

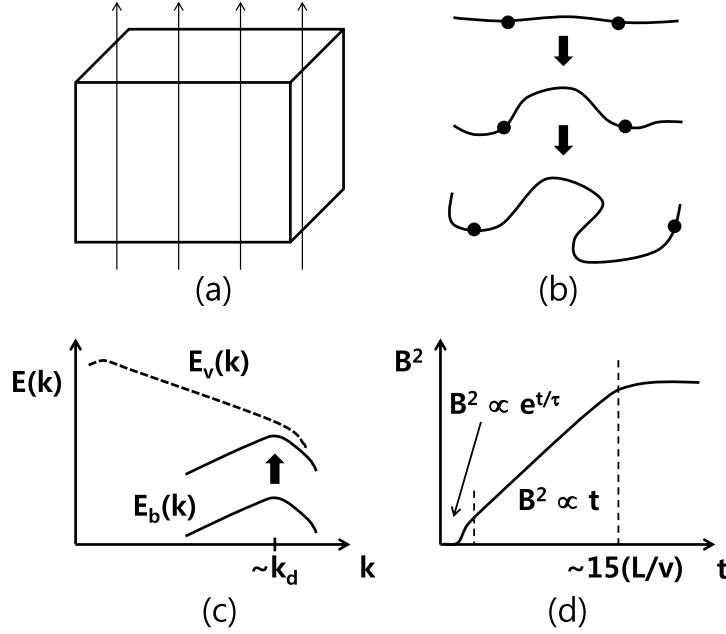


**Figure 9.** Turbulence dynamo for a uniform seed magnetic field. We assume unit magnetic Prandtl number with a very large hydrodynamic Reynolds number. (a) If the seed magnetic field is a primordial one, it can be regarded as spatially uniform or homogeneous on comoving scales of  $\sim \text{Mpc}$ . (b) When we consider two points whose separation is  $\sim l_d$ , the distance between the two point along the field line doubles after each eddy turnover time,  $\sim l_d/v_d$ , where  $v_d$  is velocity at the velocity dissipation scale  $l_d$ . Therefore, the distance grow exponentially, so does magnetic energy density. (c) Since the characteristic scale in (b) is  $l_d$ , the magnetic energy spectrum peaks near the dissipation wavenumber  $k_d$ . As time goes on, the magnetic spectrum goes up without changing the shape much. (d) In summary, the magnetic field grows in 3 steps: exponential growth, linear growth, and saturation. When the hydrodynamic Reynolds number ( $Re$ ) approaches infinity, the duration of the exponential growth stage becomes zero.

#### *Amplification of a uniform seed field*

This topic has been studied extensively in literature. In summary, growth of a uniform weak seed magnetic field in unit magnetic Prandtl number turbulence follows the following three stages (see Schlüter & Bierman 1950; Schekochihin & Cowley 2007; Cho et al. 2009; see also Cho & Vishniac 2000; Schober 2012a).

(1) The stretching of the magnetic field lines occurs most actively near the velocity dissipation scale first. This is because eddy turnover time is shortest, hence the rate of field-line stretching is highest, at the dissipation scale. Suppose that we introduce a weak uniform seed magnetic field in a turbulent medium (see Figure 9(a)). Let us select two points on a magnetic field line whose separation is of order  $l_d$ , where  $l_d$  is the velocity dissipation scale (Figure 9(b)). After approximately one eddy turnover time,  $\tau_d \sim l_d/v_d$ , where  $v_d$  is the velocity at the dissipation scale, the distance between the two points along the field line will be doubled. After approximately another eddy turnover time  $\tau_d$ , the distance between the two points along the field line will be doubled again. Therefore, magnetic field lines are stretched exponentially and, as a result, the magnetic energy density grows exponentially. Note that the typical scale of the magnetic field-line variation, which is of order  $l_d$ , does not change during the process. Therefore, the magnetic energy spectrum peaks near  $k_d$  ( $\propto 1/l_d$ ) and, as time goes on, it goes upward without changing its shape much (Figure 9(c)).

(2) As the magnetic energy spectrum moves upward, it will finally touch up the kinetic energy spectrum at the dissipation scale. Then what will happen? When the magnetic energy spectrum becomes comparable to the kinetic energy spectrum at the dissipation scale, magnetic back-reaction suppresses stretching of magnetic field lines at the dissipation scale. Due to the suppression, the exponential growth stage ends. Note, however, that stretching at scales larger than  $l_d$  is still efficient because the kinetic energy spectrum is still higher than the magnetic energy spectrum at the scales. Therefore, now the scale slightly larger than the dissipation scale becomes the most active scale for stretching. This way, the subsequent stage is characterized by a slower growth of magnetic energy and a gradual shift of the peak of the magnetic energy spectrum to larger scales (Cho & Vishniac 2000). The growth rate of the magnetic energy density at this stage turns out to be linear (Schlüter & Biermann 1950; Schekochihin & Cowley 2007).

(3) The amplification of magnetic field stops when the magnetic energy density becomes comparable to the kinetic energy density at the outer-scale of turbulence and a final, statistically steady, saturation stage begins. During the saturation stage, the peak of the magnetic energy spectrum occurs at a wavenumber a few times larger than that of the kinetic energy spectrum (Cho & Vishniac 2000).

In the vanishing viscosity (and diffusivity) limit, the duration of the exponential growth stage will be very short. Nevertheless, since the eddy turnover time at the dissipation scale is arbitrarily small in the limit, any weak seed field can grow exponentially, reach the equipartition strength at the dissipation scale, and enter the linear growth stage within arbitrarily small amount of time. Therefore, in the vanishing viscosity limit, 1) the exponential growth

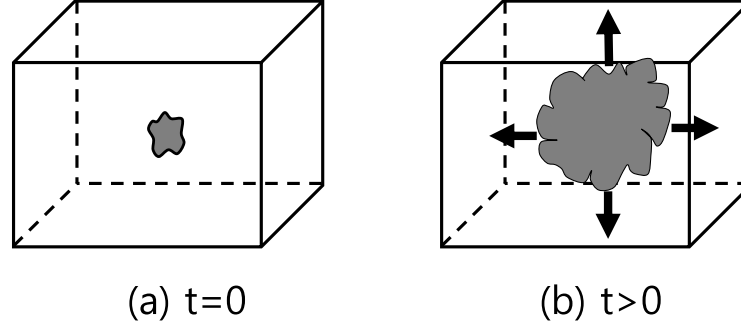


**Figure 10.** A localized seed magnetic field in a turbulent medium. (a) If the seed magnetic field is ejected from an astrophysical body, it can be spatially localized at the time of injection. (b) As time goes on, the magnetized region expands. The speed of expansion is  $\sim v$ , where  $v$  is the turbulence velocity. stage shown in Figure 9(d) becomes invisible, 2)  $B^2(t)$  shows linear growth most of the time before saturation, and 3) regardless of the strength of the initial seed field,  $B^2(t)$  follows virtually the same curve of growth when  $B^2$  is plotted in a linear scale as in Figure 9(d). According to simulations (e.g. Cho et al. 2009; Cho & Yoo 2012), the system reaches the saturation stage in  $\sim 15(L/v)$ .

#### *Amplification of a localized seed field*

Amplification of a localized seed magnetic field was studied in detail by Cho & Yoo (2012) and Cho (2013). If a seed magnetic field is localized in space, turbulent motions make the seed magnetic field transported out from the region of initial injection (Figure 10). Cho (2013) found that the rate at which the magnetized region expands is  $\sim v$ . Therefore, the *homogenization timescale* (or the magnetization timescale), the time required for the magnetic field to fill the whole system, is given by

$$t_{mag} \sim L_{sys}/v. \quad (A1)$$

If the driving scale is comparable to the size of the system,  $L_{sys}$ , then homogenization happens fast, i.e. within  $L_{sys}/L$  times the large-eddy turnover time  $L/v$ , and the subsequent evolution should be similar to that of a uniform/homogeneous seed magnetic field case (Cho & Yoo 2012)<sup>5</sup>. The whole system reaches the saturation stage within  $\sim 15L_{sys}/v$ . On the other hand, if the driving scale is less than  $\sim L_{sys}/15$ , i.e. if  $L_{sys}/L > 15$ , the magnetic field near the initial injection cite reaches the equipartition strength  $B_{eq}$  before the magnetic field fills the whole system. In this case, it takes more than  $\sim L_{sys}/v = (L_{sys}/L)(L/v)$  for the whole system to reach the saturation stage.

As in uniform/homogeneous seed field cases, as long as the strength of the seed magnetic field is sufficiently weaker than the equipartition strength, its absolute value does not matter much in the vanishing viscosity limit. First, because weak magnetic fields are passively transported and stretched by turbulent motions, the homogenization timescale  $t_{mag}$ , which is mainly determined by large-scale turbulent motions, is similar for all weak seed magnetic fields. Second, as in the uniform/homogeneous seed field cases, the strength of the weak seed fields does not affect the saturation time much. Therefore, the turbulence dynamo process should be similar for sufficiently weak localized seed magnetic fields.

#### *Observational Implications*

Since turbulence dynamo is so efficient in the vanishing viscosity limit that it is difficult to find a constraint on the strength of the initial seed magnetic field. This is true for both the primordial and the astrophysical seed magnetic fields.

However, it might be possible to tell the origin of the cosmic magnetism by observing the distribution of magnetic field in some systems. The key quantity is the homogenization timescale,  $t_{mag}$ . Suppose that a localized seed magnetic field is injected into a system. If  $t_{mag}$  is short compared with the age of the universe, the system becomes homogenized quickly and the subsequent evolution will be very similar to that of a uniform seed magnetic field. Therefore, in this case, it will be very difficult to distinguish the astrophysical and the primordial seed magnetic fields. On the other hand, if  $t_{mag}$  is longer than the Hubble time, the system has not been yet completely magnetized. Therefore, in this case, the magnetic field in the system will be very inhomogeneous.

Consider a cluster of galaxies with  $L_{sys} \sim 1$  Mpc. In this case, if  $v > 75$  km/s, which is very likely, the homogenization timescale is shorter than the Hubble time. Therefore, it will be very difficult to distinguish the primordial and the astrophysical origins of magnetic fields in clusters. On the other hand, if we consider a filament of width  $\sim 4$  Mpc, the homogenization timescale is longer than the Hubble time, if  $v < 300$  km/s. Therefore, it is possible that filaments have not been fully homogenized. If this is the case, the distribution of magnetic fields in filaments is more or less inhomogeneous.

<sup>5</sup> This result is consistent with earlier cosmological simulations. Dolag et al. (1999, 2002), for example, found that information on

the initial magnetic fields (homogeneous or chaotic) is completely wiped out during the cluster formation and simulations yield similar results.